COB-2021-0894
DESIGN, SIMULATION AND ANALYSIS OF A COAXIAL L-DED POWDER HEAD

João Victor Osório
Milton Pereira
Federal University of Santa Catarina - UFSC
joaoosorio1@hotmail.com
milton.pereira@ufsc.br

Jhonattan Guthjahr
João Antonio Wendt Dreveck
SENAI Inovation Institute for Manufacturing and Processing Laser Sistems
jhonattan.gutjahr@sc.senai.br
joao.wendt@sc.senai.br

Abstract. *In recent years, additive manufacturing technology based on Laser Directed Energy Deposition (L-DED) has attracted attention due to the growing potential for industrial development, mainly for fabrication and repair of high added value components. However, the L-DED process requires precise devices for maintenance, repair, and overhaul (MRO) goals achievement, especially in its powder fed version. Besides the laser optical system and appropriate material, the powder feeding head design stands out in process precision safety, ensuring high-quality deposition and efficient raw material use. Moreover, during the development of an L-DED powder head, it is required to achieve the expected mass flow rate, which is crucial to reach the desired powder laser melting efficiency and successful deposition effect. Analyzing the device's internal geometry and simulating variations on concentrical cones present in the nozzle outlet, the nozzle presents a variation on the powder beam final shape. Consequently, precise components geometry modification supported by Computational Fluid Dynamics analysis enables setback solving and clarifies possible issues presented on the operation. The present paper describes an unsuitable powder flow solution and its challenges, based on changes in internal geometry characteristics of the nozzle. Furthermore, correlation between head design, powder feed and CFD simulations are discussed. Finally, is shown the correlation between the alterations on the nozzle and its consequences on the diameter of the powder focal point and the focal distance. Furthermore, methodology presented in this paper can be applied for different situations relating L-DED powder heads developed and its entire process efficiency.*

Keywords: *Laser Directed Energy Deposition, Additive Manufacturing, Laser Cladding, Laser Powder head.*

1. INTRODUCTION

One of the most wanted goals of engineering is the development of technologies to increase the service life of machine components. In operation, the highest rate of wear is found in the local sections of working surfaces, in which is necessary to produce precise reconditioning without affecting other characteristics and properties of the component (Grigoryants *et al*., 2015). For this purpose, an important branch of Additive Manufacturing, Laser Directed Energy Deposition (L-DED) with coaxial powder feeding is used. The schematic of L-DED processes working space can be seen in Figure 1 (Yan *et al*., 2017). The powder is fed to the processing zone coaxially in relation to the laser beam to receive a high energy density and create a melting pool on substrate material where occurs the cladding of surface (Tabernero *et al*., 2010). This technology allows the production of high-performance coatings, remanufacturing of damaged parts, and building of tridimensional products with complex structures (Zhang *et al*., 2021).

Aerospace, automotive, naval and oil and gas industries are potential users of this technology, due to the possibility of producing precise maintenance, repair, and overhaul of components, with high-added value. Therefore, tools and methods with great efficient performance allied to high quality materials are required, as L-DED and its processed metal alloys (Korsmik *et al*., 2017).

The powder capture efficiency of L-DED process is determined by the process parameters and hardware configurations, mainly based on the nozzle geometrical characteristics. The nozzle, also called the head, is the main responsible for generating homogeneous and concentrated powder stream and makes it possible to deposit materials on the surfaces in a wide range of dimensions and with different materials, without compromising the efficiency of deposition (Grigoryants *et al.*, 2015). The deposited beads geometry is dependent on the melt pool geometry and the powder distribution, which is determined by the particles trajectories during deposition, and is directly affected by the geometry of the nozzle (Grigoryants *et al.*, 2015; Yan *et al.*, 2017).

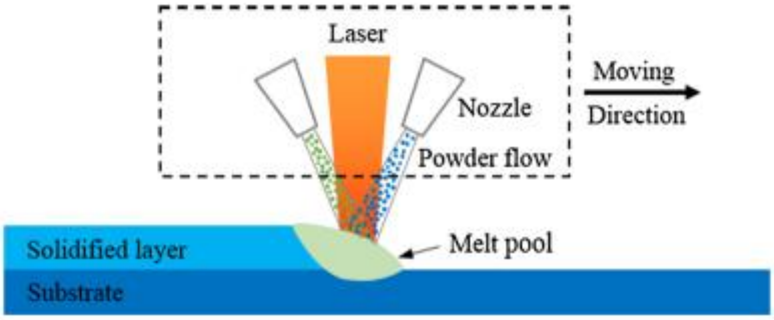

Figure 1. Schematic of a L-DED process with coaxial injection powder nozzle (Yan *et al*., 2017)

Powder nozzles with coaxial powder feed are characterized by a high stability of gas-powder flow, due to the powder being supplied through the cavity between two or three conical surfaces. The internal nozzle shape provides uniformity on the powder deposition, resulting in efficient coatings in any spatial position and direction (Grigoryants *et al.*, 2015).

Nozzle geometry and operating conditions have prominent importance in L-DED powder deposition to increase the process efficiency and to ensure the quality of the clads (Arrizubieta *et al*., 2014). In this case, dealing with a ring coaxial nozzle, the particles transport mechanisms and the characteristics of powder flow shape mainly depend on the ring structure that composes the concentric internal cones (Melo, 2015; Zhang *et al.*, 2021). Furthermore, powder particle transport is a complex physical process involving energy, momentum and mass transport, so detailed calculation methods and numerical simulations are required for powder flux description (Arrizubieta *et al*., 2014; Ibarra-Medina & Pinkerton, 2010; Yan *et al.*, 2017; Zhang *et al*., 2021).

In this study, a Computational Fluid Dynamics (CFD) model was applied to describe the powder flux behavior, which is characterized and affected by the ring geometrical structure in concentric internal nozzle cones. The present paper aims to describe and discuss the influence of a variation in geometrical coaxial nozzle parameter on gas-powder flux and its interactions with particles velocity, powder flow distribution and powder flux focal point position.

2. NOZZLE AND SIMULATION

2.1 Nozzle

The coaxial nozzle under study in this paper was previously designed and manufactured by Precision Engineering Laboratory group in collaboration with SENAI Innovation Institute for Manufacturing Systems and Laser Processing (Pereira *et al*., 2019) and is presented in Figure 2.a). Figure 2.b) shows the nozzle concentric cones (A and B) and the resulting gas-powder channel to allow the flow through. Four tubular entrances (C) equally spaced on structure give the way to form an annular channel for powder and carrier gas feeding into the nozzle, carried to where the ring ends, and the powder is then directed to substrate. The shape of the ring produced by the concentric cones (D), also called as gap and its adjustable.

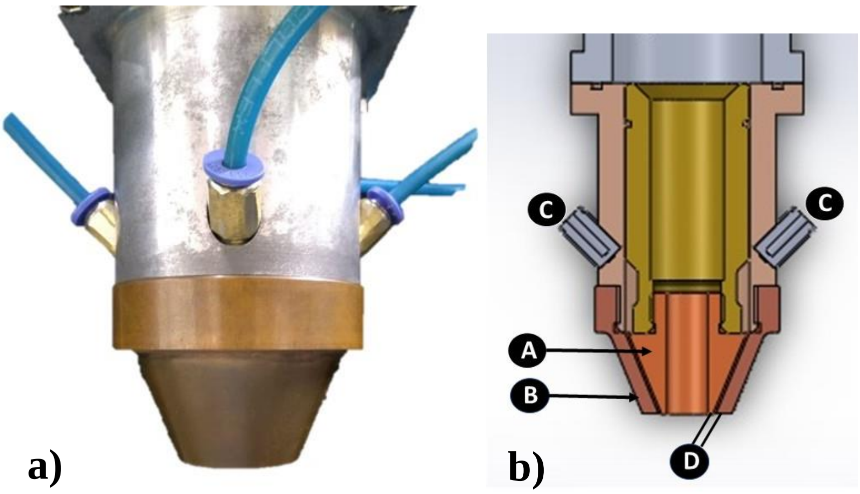

Figure 2. Coaxial nozzle external view (a) and its sectional representation view (b)

2.2 Mathematical model

Considering an L-DED nozzle design, the powder particle concentration distribution on the nozzle outlet is one of most important process parameters. Its relevance is related with the desire of laser beam focus and the powder stream focus begin coincident or, at least, relatively close to each other. In this way the powder has an efficient usage, avoiding resources wastage (Pereira *et al*., 2019).

In L-DED powder processes, the powder stream is constituted of two phases, namely the carrier and shielding gas as continuous phase and the powder particles as discrete phase. The continuous phase modelling relies on Navier-Stokes equations and standard κ-ε turbulence model (Pitchard and Mitchell, 2011; Pereira *et al*., 2019; Tabernero *et al*., 2010).

The main group of equations for κ-ε turbulence model are shown in equation 1 and equation 2. Equation 1 presents the conservation of kinetic energy of turbulence in terms of k, while equation 2 presents conservation or dissipation of kinetic energy of turbulence in terms of ε.

$$\frac{\partial}{\partial x_i}(\rho k u_i) = \frac{\partial y}{\partial x_j}\left[\left(\mu + \frac{\mu_t}{\sigma_k}\right)\frac{\partial k}{\partial x_j}\right] + Gk + Gb - \rho \tag{1}$$

$$\frac{\partial}{\partial x_i}(\rho \varepsilon u_i) = \frac{\partial y}{\partial x_j}\left[\left(\mu + \frac{\mu_t}{\sigma_\varepsilon}\right)\frac{\partial \varepsilon}{\partial x_j}\right] + C1_\varepsilon \frac{\varepsilon}{k}(Gk + Gb) - C2_\varepsilon \rho \frac{\varepsilon^2}{k} \tag{2}$$

At the same, Gk (equation 3) quantifies the effect of the mean velocity gradients on the turbulence kinetic energy generation and Gb (equation 4) is the buoyancy role on the turbulence kinetic energy generation.

$$Gk = \mu_t \left(\frac{\partial uj}{\partial xi} + \frac{\partial ui}{\partial xj}\right)\frac{\partial ui}{\partial xj} \tag{3}$$

$$Gb = -gi \frac{\mu_t}{\rho Prt} * \frac{\partial p}{\partial xi} \tag{4}$$

The variables xi and ui represent respectively the position and velocity, ρ is the gas density and μ is the molecular viscosity. $C1_\varepsilon = 1.44$, $C2_\varepsilon = 1.92$ and $\sigma_\varepsilon = 1.3$ are empirical constants. Also, gi represents the gravity force actuating on the situation (Pitchard and Mitchell, 2011).

The powder solid particles tracking is calculated in a Lagrangian reference frame, considering a force balance at the particles individually, which its integration gives the particle trajectory. For a given particle, the force balance in x axis direction can be written as described in equation 5.

$$\frac{du_p}{dt} = F_D(u - u_p) + gx\left(\frac{\rho_p - \rho}{\rho_p}\right) + F_x \tag{5}$$

In equation 5 u_p is the particle velocity, u is the fluid velocity, ρ is density of fluid, ρ_p is particle density and F_D is the drag force actuating. In presented cases, p represents values assigned to the particles. Also, gx represents the gravity force actuating on the situation. On right side of equation, the second term represents the drag force per unit of particle mass and, at end, *Fx* is the particles acceleration term. Equation 6 describes F_D according to μ, representing fluid molecular viscosity, d_P as particle medium diameter, Re is the Reynolds flow number and *Cd* is the drag coefficient, which is obtained for empirically estimation (Tabernero *et al*., 2010).

$$F_D = \frac{18\mu}{\rho_P {d^2}_P}\frac{C_D Re}{24} \tag{6}$$

2.3 Computational Fluid Dynamics model

To consolidate the mathematical model, the Computational Fluid Dynamics model is structured and its results are discussed. Like the model presented by Zhang et al., (2021), as shown in Figure 3, the model used in this paper includes two domains for examination. The first domain is the nozzle flow channel geometric model, which expresses insider nozzle powder flow and its orientation for final ring shape (influenced by the cones gap) and outside area. Powder particles, including carrier gas, are piped by four routes into the annular region of the nozzle, represented by the inlet.

The second domain is an extended cylinder with an entrance size of 35 mm. External cylinder sizes are 50mm in diameter and 100 mm high. This structure is used to study the particles transport outside the nozzle and powder-gas flow behavior, including particles' velocity and powder flow focal point geometrical location.

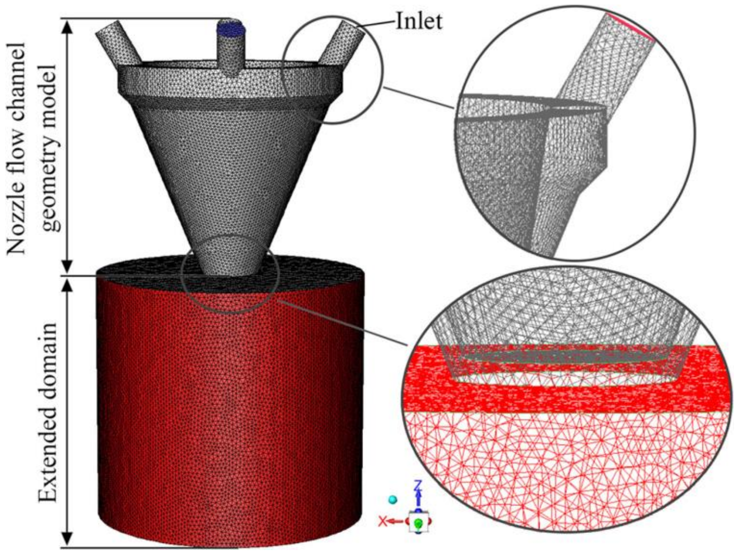

Figure 3. CFD simulation model of powder flow (Zhang *et al*., 2021)

The model applied in this work uses the discrete phase method (DPM) for evaluating the particles dynamics interacting with the surroundings. One-way coupling was considered since the discrete phase is very dilute. This assumption can be made when the volumetric fraction of the disperse phase is lower than 10% and it is valid considering the common values of mass flow rate used during processing. One-way coupling considers the effect of the continuous phase flow over the discrete phase and disregards the effect of the discrete phase over the continuous phase, also does not consider the physical chock between individual particles. Due to this, the mass flow rate is not considered as a variable and the main concern is to predict the particles ejection trajectories. Three different gap parameters are considered, 0,3 mm, 0,6 mm and 1,0 mm. For other parameters used in simulation, table 1 shows the shielding gas flow rate, carrier gas flow rate, and particles diameter average size, based on normal statistical distribution.

Table 1. Experimental parameters used in CFD simulation.

Carrier gas flow rate	**Shielding gas flow rate**	**Particles average diameter size**
5 L/min	15 L/min	100 µm

The values used in the simulation are based on extensive literature research and previous experiences. Simulation results are obtained applying a variation on gap sizes, which comprehend sizes of 0,3 mm, 0,6 mm and 1,0 mm.

3. RESULTS AND DISCUSSION

Simulation results are based on particles velocity, which is presented as a colors variation and expressed on the figure’s legend on the left side. Due to that, it is possible to notice that this velocity is increased directly with gap narrowing. The geometrical influence caused by the gap variation affects directly the final pressure on powder exit. While the available area is reduced and the flow rate is kept the same, the pressure must increase to assure the physical relation. Therefore, is possible to detect higher velocities on smaller gaps.

Besides the velocity alteration, it is also possible to detect a variation on the geometrical position of the powder stream focal point, representing the highest particles concentration. Figures 4, 5, and 6 show this relation precisely, in order to show the positions on 0,3 mm, 0,6 mm, and 1,0 mm gap, respectively.

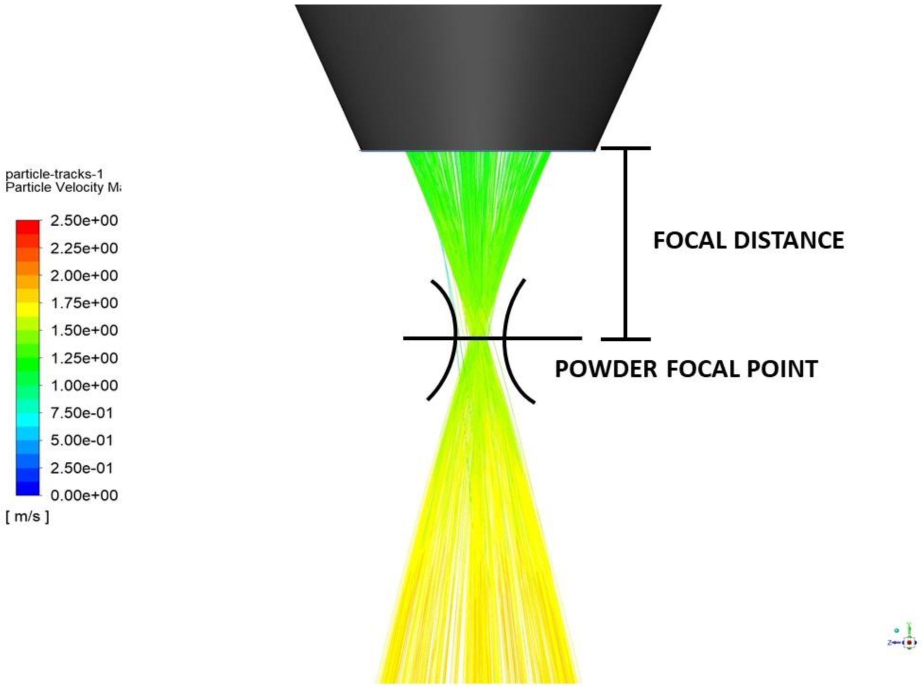

Figure 4. Powder-gas flow focal point position on 0,3 mm gap

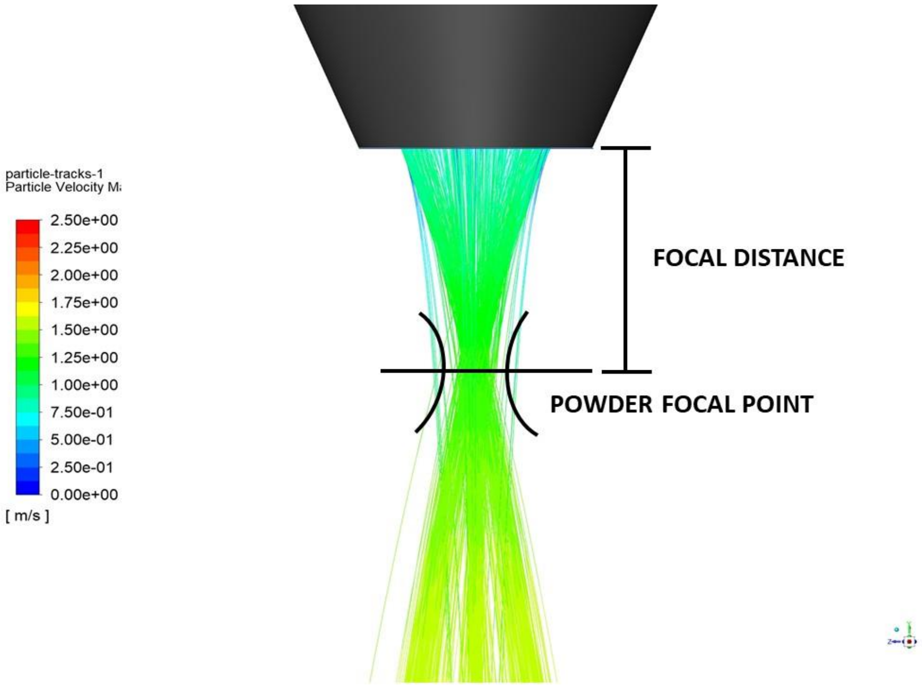

Figure 5. Powder-gas flow focal point position on 0,6 mm gap

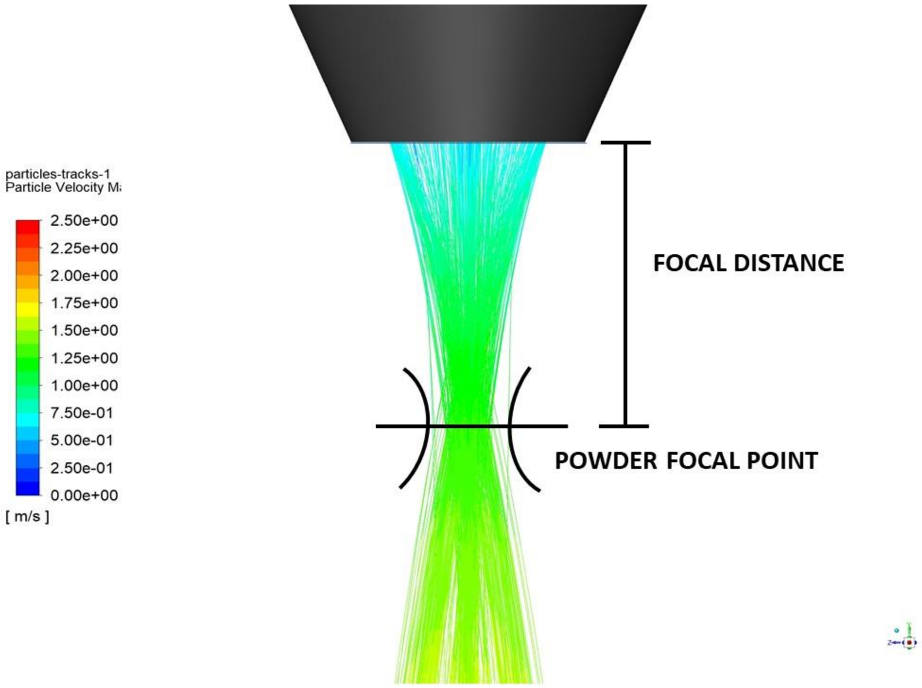

Figure 6. Powder-gas flow focal point position on 1,0 mm gap

A higher value on gap results in a lower geometrical concentration for powder stream, which reflects on different focal point positions in each condition. That makes possible a bigger powder amount letting out the nozzle towards substract. The gap increment is directly proportional to the distance from the focal point and the nozzle exit.

Also, is possible to notice that the diameter of focal point has the same increasing behavior as the gap. The amount of powder ejected by the 1,0 mm gap results in a bigger diameter on focal point, in opposition with 0,3 mm gap, which represents a lower powder focus diameter. Thereby, Figures 7 and 8 express the variation of distance from the powder focal point to the nozzle outlet showing that as gap is increased a variation of the diameter size of the powder focal point increases accordingly.

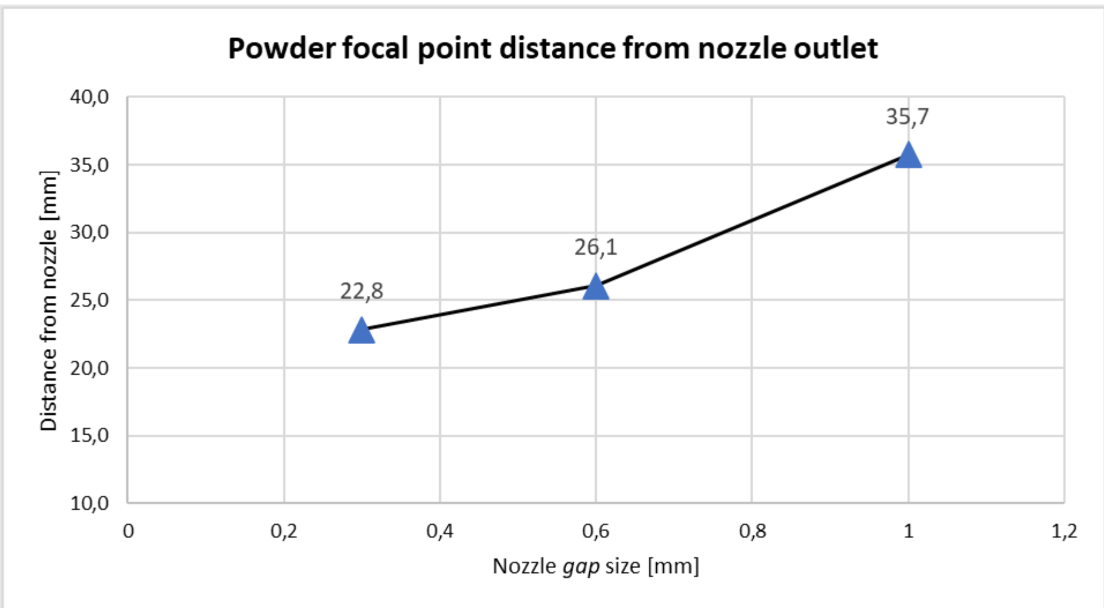

Figure 7. Variation of distance of powder focal point from nozzle outlet in according to gap size increasing

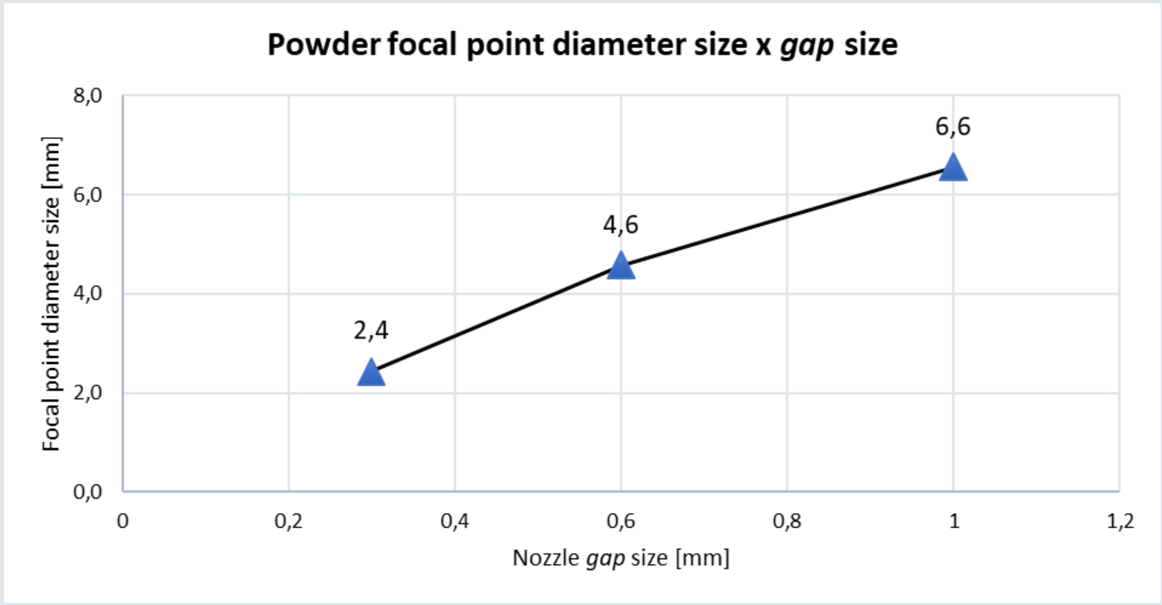

Figure 8. Variation of diameter size of powder focal point in according to gap size increasing

Figures confirmed quantitatively the modification of powder stream behavior related to powder flow distribution and shape. The distances between geometrical powder focal point location and nozzle final gap, on the range of 0,3 mm gap to 1,0 mm gap, presented the variation of 22,8 mm on the minor gap, 26,1 mm on the intermediate gap and 35,7 mm on the larger gap. As expected, it was observed an increasing on the distance's values, as it was showed on Figures 4, 5, and 6.

The powder focal point diameter size started at 2,4 mm with a 0,3 mm gap, 4,6 mm on 0,6 mm gap and up to 6,6 mm on 1,0 mm gap size. Also, this behavior is expected, as showed qualitatively on Figures 4, 5 and 6. This increase in terms of focal diameter presents dependance, directly influenced by the size of the nozzle gap. One must also mention that there is a limit in the selection of the lower gap value, depending on the powder particle mean size. Under a gap value, the powder will no longer flow through the gap, causing the obstruction.

4. CONCLUSIONS

In this work it is possible to observe the influence of the L-DED powder nozzle internal geometry on the powder-gas stream. Increasing the gap size results in a lower particle velocity, detachment of powder focal point, and a lower concentration of powder particles on the focal point, increasing its respective diameter.

The numerical theoretical behavior of powder-gas stream has corresponded with the presented in computational simulation. The method applied in this work is useful to predict and study geometrical characteristics of powder stream, due to nozzle different parameters.

Increasing the gap and applying the same process conditions made it possible detect a consequent growing on the distance from the nozzle to the powder focal point and in the powder focal point diameter. The values resulted in focal distance behavior presented considerable correlation, like the one occurred with the focal point diameter.

This work shows the strong relation between shape of the gap on final cones in a L-DED nozzle and its influence on powder-gas beam physical and geometrical behavior.

5. ACKNOWLEDGEMENTS

The authors of this paper acknowledge to Precision Engineering Laboratory, located in Federal University of Santa Catarina, Florianópolis-SC and SENAI Innovation Institute for Manufacturing Systems and Laser Processing, located in Joinville-SC.

6. REFERENCES

Arrizubieta, J. L., Tabernero, I., Exequiel Ruiz, J., Lamikiz, A., Martinez, S., and Ukar, E. (2014). Continuous coaxial nozzle design for LMD based on numerical simulation. *Physics Procedia*, *56*(C), 429–438.

Pitchard, P. J., & Mitchell, J. W. (2011). Fox and McDonald's introduction to fluid mechanics (7th ed.). John Wiley & Sons.

Grigoryants, A. G., Tretyakov, R. S., Shiganov, I. N., and Stavertiy, A. Y. (2015). Optimization of the shape of nozzles for coaxial laser cladding. *Welding International*, *29*(8), 639–642.

Ibarra-Medina, J., and Pinkerton, A. J. (2010). A CFD model of the laser, coaxial powder stream and substrate interaction in laser cladding. *Physics Procedia*, *5*(PART 2), 337–346.

Korsmik, R. S., Turichin, G. A., and Babkin, K. D. (2017). Laser cladding technological machine. Investigation of efficiency of various nozzles design. *Journal of Physics: Conference Series*, *857*(1).

Melo, L. (2015). *Powder Jet Particle Density Distribuition Analysis and Qualification for the LASER Metal Deposition*, M.Sc. thesis, POSMEC, Federal University of Santa Catarina, Brazil.

Pereira, M., Fraga, G., Gutjahr, J., and Osório, J. V. E.-H. M. (2019). LMD-Powder Head: Design, Manufacturing and Validation. *International Congress on Applications of Lasers & Electro-Optics*.

Tabernero, I., Lamikiz, A., Ukar, E., López De Lacalle, L. N., Angulo, C., and Urbikain, G. (2010). Numerical simulation and experimental validation of powder flux distribution in coaxial laser cladding. *Journal of Materials Processing Technology*, *210*(15), 2125–2134. http://dx.doi.org/10.1016/j.jmatprotec.2010.07.036

Yan, J., Battiato, I., and Fadel, G. (2017). Design of Injection Nozzle in Direct Metal Deposition (DMD) Manufacturing of Thin-walled Structures Based on 3D Models. *International Journal of Advanced Manufacturing Technology*, *91*(1–4), 605–616.

Zhang, J., Yang, L., Li, Z., Zhang, Q., Yu, M., Fang, C., and Xiao, H. (2021). Transport phenomenon, flow field, and deposition forming of metal powder in the laser direct deposition with designed nozzle. *International Journal of Advanced Manufacturing Technology*, *114*(5–6), 1373–1383.

7. RESPONSIBILITY NOTICE

The authors are the only responsible for the printed material included in this paper.